
**Separation Science and Technology**
Publication details, including instructions for authors and subscription information:
http://www.informaworld.com/smpp/title~content=t713708471

# Kinetics and Equilibrium Sorption Models: Fitting Plutonium, Strontium, Uranium, and Neptunium Loading on Monosodium Titanate (MST)

F. F. Fondeur[a]; D. T. Hobbs[a]; M. J. Barnes[a]; T. B. Peters[a]; S. D. Fink[a]
[a] Savannah River National Lab, Westinghouse Savannah River Company, Aiken, South Carolina, USA

**To cite this Article** Fondeur, F. F. , Hobbs, D. T. , Barnes, M. J. , Peters, T. B. and Fink, S. D.(2006) 'Kinetics and Equilibrium Sorption Models: Fitting Plutonium, Strontium, Uranium, and Neptunium Loading on Monosodium Titanate (MST)', Separation Science and Technology, 41: 11, 2429 — 2445
**To link to this Article: DOI:** 10.1080/01496390600745495
**URL:** http://dx.doi.org/10.1080/01496390600745495

*Separation Science and Technology*, 41: 2429–2445, 2006

ISSN 0149-6395 print/1520-5754 online
DOI: 10.1080/01496390600745495



# Kinetics and Equilibrium Sorption Models: Fitting Plutonium, Strontium, Uranium, and Neptunium Loading on Monosodium Titanate (MST)

**F. F. Fondeur, D. T. Hobbs, M. J. Barnes, T. B. Peters, and S. D. Fink**
Savannah River National Lab, Westinghouse Savannah River Company, Aiken, South Carolina, USA

**Abstract:** The Dubinin-Astashov (DA) isotherm parameters for U, Pu, Sr, and Np have been updated to include additional data obtained since the original derivation. The DA isotherms were modified to include a kinetic function derived by Rahn to describe sorbate loading from the beginning of sorption up to steady state. The final functions describe both kinetic and thermodynamic sorption.

**Keywords:** Actinide, sorption, sodiumtitanate

## INTRODUCTION

The salt waste processing facility (SWPF) and the actinide removal process (ARP) will treat salt solution from the Tank Farm that contains actinide levels in excess of the saltstone waste acceptance criteria (WAC). Saltstone is the name given to the mixture of salts (from the supernate) and grout (cement). The SWPF is a future facility where cesium will be removed from the supernate (salt solution). The ARP is a future facility where strontium, plutonium, uranium, and neptunium will be removed to an acceptable concentration level for mixing with grout. The grout will be poured into

Received 23 October 2005, Accepted 22 March 2006
Address correspondence to F. F. Fondeur, Savannah River National Lab, Westinghouse Savannah River Company, 773A, B124, Aiken, SC 29808, USA. Fax: 803-725-2777. E-mail: fernando.fondeur@srnl.doe.gov

vaults to be built below the ground. The supernate treatment includes removal of $^{90}Sr$ and alpha-emitting ($^{238,239,240}Pu$, $^{237}Np$) radionuclides from salt solution. The baseline technology features contacting the liquid waste with a sorbent (monosodium titanate (MST)) in a tank (batch mode). The rate and extent of Pu removal by MST sets the SWPF footprint and establishes cycle time and throughput for the ARP. To increase throughput and optimize the process, a predictive tool for actinide removal with MST is required. To this end, a previous study fitted several isotherm functions to existing actinide on MST sorption data (1). That study identified the Dubinin-Astashov (DA) function fitted the sorption data well.

Since the completion of that work, new actinide adsorption data has been collected (2, 3). This paper incorporates the new data with the previous databank and recalculates the Dubinin-Astashov parameters. In addition, this paper develops a predictive tool for estimating actinide removal from liquid waste as a function of time. The final equation predicts both actinide concentration as a function of time and equilibrium (steady state) concentrations.



## EXPERIMENTAL

We recently conducted additional MST sorption tests to generate 44 data points. The new tests covered concentration ranges not previously studied. This data was checked for mass balance consistency (what is on the MST and remains in solution must equals the initial starting amount of radionuclide). The data was further checked for sorption competition (for example if variations in the concentration of one radionuclide affect the sorption of others). We performed correlation tests between the equilibrium sorption of a radionuclide on MST and the concentration of the remaining radionuclides. A negative correlation result is evidence of lack of sorption competition. This implies that the Sr and actinides are sorbing on different sites in MST. This allows fitting sorption data with functions that only include the radionuclide being studied without considering the presence of the other radionuclides. The shape of the curve, representing the amount of actinide loaded on MST and the remaining concentration of actinide in solution, is initially linear and then it reaches a steady state value as a function of actinide concentration in solution.

The equilibrium sorption data was re-fitted with a DA function. The fitting procedure included a non-linear square fitting (minimizing the Sum of Square Errors) that used the Newton-Ralphson searching criteria. Convergence was reached when either the objective (the sum of the square difference between the prediction from the Dubinin-Astashov function and the sorption data), or parameters changes or the gradient of change was less than $10^{-6}$. A similar criterion was used for fitting the kinetic sorption data to different kinetic functions.

To predict the amount of MST per unit volume of supernate (per liter) needed for a given DF value, we combined the Dubinin-Astashov

equation with the mass balance equation. The Dubinin-Astashov equation follows (4, 5).

$$q_{equilibrium} = q_{equilibrium}^{maximum} \times e^{-((RT/E)\,Ln(S/[actinide]_{equilibrium}))^n} \tag{1}$$

In this expression, $q_{\max}$ is the maximum strontium or actinide loaded on MST (given in μmole/g), $E$ is the adsorption energy and $S$ is the maximum radionuclide concentration in solution tested. We coupled equation (1) to the mass balance equation between actinide in solution, on MST and the original concentration to generate equation (2).

$$q_{equilibrium} = \frac{[\text{sorbate}]_{initial}}{[MST]} \times \left(1 - \frac{1}{DF}\right) \tag{2}$$

In this expression, $[\text{sorbate}]_{initial}$ stands for the initial actinide concentration with μmolar units (before MST addition), [MST] is MST concentration in grams/L and $DF$ stands for decontamination factor. Combining equations (1) and (2) leads to the following expression.

$$[MST] = \frac{[\text{sorbate}]_{initial}}{q_{equilibrium}} \times \left[1 - \frac{1}{DF_{equilibrium}}\right] \times e^{a \times [Ln(S \times DF_{equilibrium}/[sorbate]_{initial})]^b} \tag{3}$$

From equation (3) given an initial sorbate concentration and desired decontamination factor, the MST concentration (grams/L) is easily obtained. Conversely, given an initial concentration of sorbate and MST concentration, the equation also provides the resulting decontamination factor.

To predict the "DF" value as a function of time, we rearranged the mass balance equation in terms of the equilibrium DF and sorbate loadings at equilibrium and time "t" as shown in equation (4).

$$DF(t) = \frac{1}{1 - (1 - (1/DF_{equilibrium})) \times (q(t)/q_{equilibrium})} \tag{4}$$

In this expression "$q(t)/q_{equilibrium}$" (the extent of loading to equilibrium) is the kinetic function describing how much sorbate loads on MST as a function time. One of the purposes of this work is to find a kinetic adsorption function for actinide sorption on MST that can be inserted in equation (4). A literature search identified several kinetic functions for adsorption process. Table 1 provides a list of the functions evaluated in this report. Table 2 provides the kinetic expressions for each of the functions listed in Table 1. For example, inserting the Rhan function to equation (4) yields a temporal DF equation as shown in equation (5).

$$DF(t) = \frac{1}{1 - (1 - (1/DF_{\text{equilibrium}})) \times [1 - e^{-k \times t^n}]} \tag{5}$$

***Table 1.*** The kinetic functions considered for fitting actinide loading

| Model | Parameters | #Mathematical operations of operations | Formula | Reference |
|---|---|---|---|---|
| First order | 2 | 5 | $q = q_{equilibrium}\,(1 - e^{-kt})$ | (6(a)) |
| Second order | 2 | 5 | $q = q_{equilibrium}\,(1 - 1/(1 + kt))$ | (6(b)) |
| Ritchie | 3 | 6 | $q = q_{equilibrium}\,(1 - (1/(1 + kt))^{n})$ | (5) |
| Elovich | 2 | 4 | $q = q_{equilibrium} Ln\,(at + 1)$ | (7) |
| Diffusion limited | 1 | 2 | $q = bt^{1/2}$ | (8, 9, 11, and 12) |
| Power | 2 | 2 | $q = bt^{a}$ | (6) |
| Rahn | 3 | 6 | $q = q_{equilibrium}\,(1 - \exp(-kt^{n}))$ | (4,10) |
| Shrinking core model | 3 | 6 | $t = a[1 - bx^{2/3} + cx]$ | (6(b)) |
| Rudzinski | 4 | 11 | $q = q_{equilibrium}\,(a \times \mathrm{Arctan}(bt))^{c}/(1 + (a \times \mathrm{Arctan}(bt))^{c})$ | (7) |

[a]In this table "$k$" stands for the rate constant, "$t$" stands for time, and "$a$, $b$, and $c$" are constants.



The current strategy is to compute the equilibrium DF using equation (3) given an initial sorbate concentration and MST concentration or the MST concentrations given an initial sorbate concentration. Then the temporal changes of DF are computed using equation (4) (or 5, for example). A diagram of the calculation steps required for predicting DF as a function time is shown in Fig. 1.

When loading is controlled by both diffusion and adsorption, a non-analytical solution (by numerical integration) can be obtained. Only in the case of flux-controlled loading at the surface of MST, an analytical solution can be obtained as shown below.

$$\begin{aligned} &\frac{dq}{dt} = D\frac{\partial C}{\partial X} \text{ at the surface.} \\ &\frac{\partial C}{\partial X} = \frac{C_{bulk}}{\sqrt{\pi D t}} \text{ for semi} - \text{infinite plane diffusion} \\ &q = \frac{2D^{1/2}C_{bulk}}{\pi^{1/2}}t^{1/2} \end{aligned} \tag{6}$$

In this expression, $D$ stands for diffusivity, $C_b$ stands for the bulk concentration of the sorbate in solution and $t$ stands for time.

Researchers felt the lists of function listed Table 1 were sufficient to fit the data without the need for using rigorous numerical solutions to the

***Table 2.*** Rate of loading equations for the kinetic expressions[a]

| Model | Kinetic expression for rate of loading dq/dt | Reference |
|---|---|---|
| First order | $k(q_{exp} - q)$ | (6(a)) |
| Second order | $k(q_{exp} - q)^2$ | (6(b)) |
| Ritchie | $k(q_{exp} - q)^n$ | (5) |
| Elovich | $\exp(-bq)$ | (7) |
| Rahn | $k(q_{exp} - q)/t^{\alpha}$ | (4, 10) |
| Shrinking core model | $D(\partial C/\partial X)_{MST}$ | (6(b)) |
| Rudzinski | $k(q_{exp} - q)^{\alpha}/q^{\alpha}$ | (7) |
| Diffusion | $D(\partial C/\partial X)_0$ | (8,9, 11 and 12) |

[a]Power model is an empirical function for fitting sorption data that did not originated from a kinetic expression.



coupled diffusion-adsorption kinetic equation. Table 1 presents a set functions that covers both diffusion-limited sorption (both in solution and in the MST) and reaction controlled sorption (for example 1st and 2nd order reactions). Please note that successfully fitting sorption data

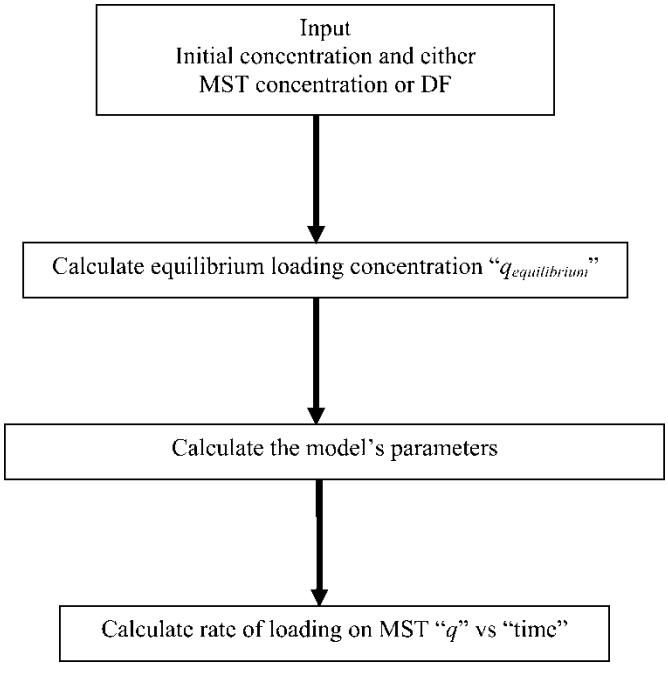


***Figure 1.*** Schematic of the calculation step needed to predict DF as a function of time.

with an exponential function does not necessarily implies first order rate sorption. Mathematical analysis of a sorption test carried under the conditions of a boundary layer around the sorbent also predicts an exponential function.

Researchers also evaluated the correlation coefficient ($r^2$) and standard error (SE) were computed to show the goodness of the fit. The $r^2$ and SE definitions follow.

$$R^2 = \frac{\sum (\text{Experiment value} - \text{Model prediction})^2}{\sum (\text{Experiment value} - \text{Mean of experiment values})^2} \quad (7)$$

$$SE = \sqrt{\frac{\sum (\text{Experiment value} - \text{Model prediction})^2}{\#\text{ of data points} - \#\text{ of parameters in the model}}} \quad (8)$$



## RESULTS

### Recalculation of the Equilibrium Dubinin-Astashov Parameters and Adsorption Enthalpy

Researchers added the more recent data on strontium and actinide sorption with the previous dataset and re-calculated new DA parameters as described in the Experimental section. The DA expressions for Sr, Pu, U, and Np are shown in equations (9–12), respectively. All sorbate concentrations are shown in units of micromoles per liter (μM) and loadings of sorbates onto MST in units of micromoles per gram of MST (μmole/g). Equations (9–12) represent the best DA function fit to a database that contains 3 different temperatures (25°C, 45°C and 65°C). This is a typical temperature range in the actinide removal process. Figures 2, 3, 4, and 5 show the Strontium, Uranium, Plutonium, and Neptunium loading on MST. Figures 2 through 5 also show the predictions from the DA function and the degree of fitting as determined from the square of the correlation coefficient. An inspection of Fig. 2 through 5 reveals that Uranium (Fig. 2), Plutonium (Fig. 3), Strontium (Fig. 4) and Neptunium (Fig. 5) loading data shows a large increase in loading after an initial plateau is reached. The large loading increase may be an indication of multilayer formation. Since Uranium, Plutonium, and Neptunium extensively load on MST, they do not compete for the same sorption sites on MST. In a previous report, the Strontium and actinide sorption energy was measured. From the sorption energy, it was concluded that only Uranium and Neptunium formed multilayers on MST (for example Uranium precipitating or sorbing on an Uranium rich surface). The additional data point in Fig. 3 is new evidence that Plutonium forms multilayer on MST.

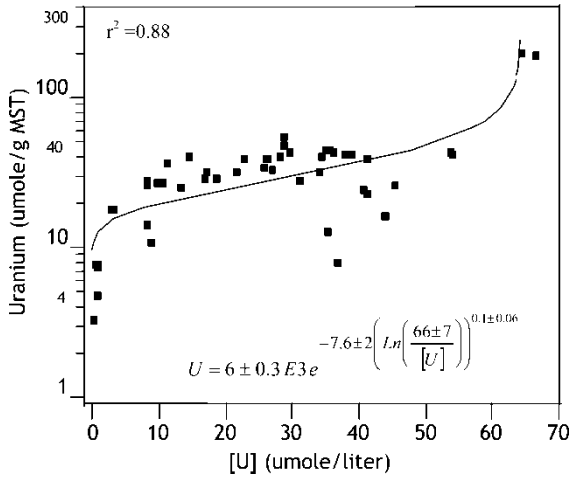


***Figure 2.*** A comparison between the DA function model and the U loading data on MST.

Strontium

$$\text{Loaded } Sr_{equilibrium} = 27.4 \pm 4\; e^{-0.2\pm0.03\times(Ln\;(0.8\pm0.01/[Sr]))^{3.6\pm0.3}} \quad (9)$$

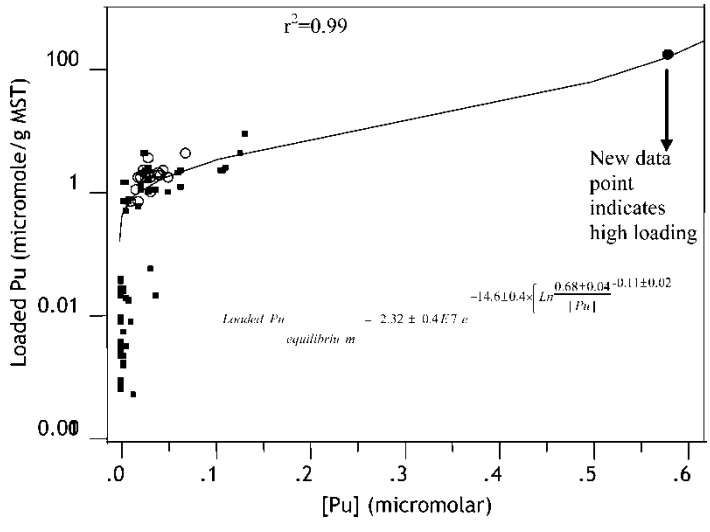


***Figure 3.*** A comparison between the Pu loading data on MST and DA modeling. The ordinate axis is displayed in logarithm scale to show the new data point that indicates high loading.

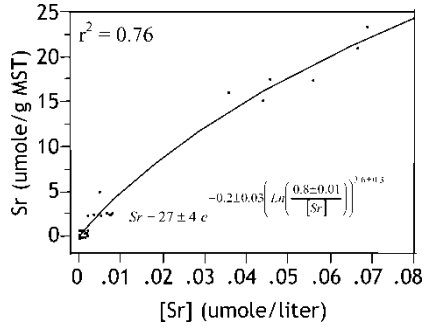


***Figure 4.*** A comparison between the Sr loading data on MST and the output from the DA model.

Plutonium

$$\text{Loaded } Pu_{equilibrium} = 2.32 \pm 0.4E7e^{-14.6\pm0.4\times[Ln(0.68\pm0.04/[Pu])]^{0.11\pm0.02}} \quad (10)$$

Uranium

$$\text{Loaded } U_{equilibrium} = 6E4 \pm 3E3\ e^{-7.6\pm1.9\,(Ln(66\pm7/[U]))^{0.1\pm0.06}} \quad (11)$$

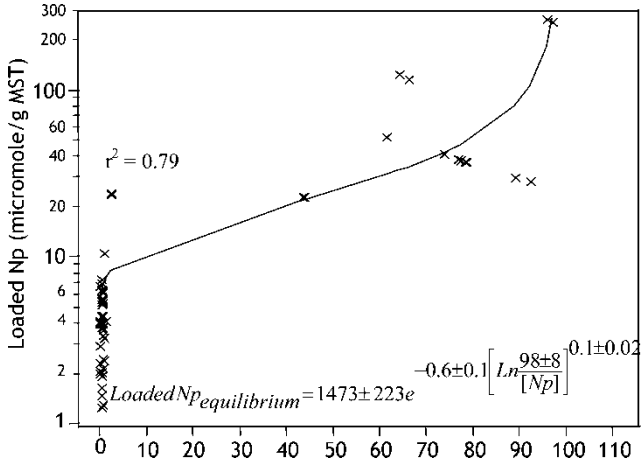


***Figure 5.*** A comparison of the output from the DA function and the Np loading data on MST.

Neptunium

$$\text{Loaded } Np_{equilibrium} = 1473 \pm 223e^{-0.6\pm0.1[Ln(98\pm8/[Np])]^{0.1\pm0.02}} \quad (12)$$

## Model Discrimination between the Kinetic Functions

Discrimination analysis focused on the Sum of Square Errors for Strontium and radionuclides. Table 3 list the resulting SSE values from fitting each function to the loading data of each actinide. We prefer that a single kinetic function provides a good fit for all four sorbates. Visual inspection of Table 3 revealed that the 1st order, 2nd order, and Diffusion-limited models exhibited large residual errors. The Rudzinski model was not considered further because of the large number of mathematical operations and sensitivity to changes in the coefficient variations. Although both the Elovich and Power function fitted the uranium data best, loading with these functions are never expected to reach steady state. Recall one function contains an exponent and the other a power of 10. The Sr loading data always reached steady state under several different initial conditions ruling out the Elovich and Power functions for fitting. Therefore, we excluded the Elovich and Power kinetic functions for further consideration.

The remaining two models, Rhan and Ritchie, had similar fitting performance. We also considered the behavior of the rate constants derived from both of these models with varying MST concentration and initial sorbate concentrations. We observed that the initial rate of sorbate loading ($dq/dt$) was the same under various different conditions (different initial actinide and strontium concentrations) as shown in Figs. 6 to 7. This is evidence that the sorption process is reaction control instead of diffusion control. Since the rate of loading appears not to be a function of the final equilibrium loading, the expression in equation (13) indicates that the rate constant should decrease with increasing equilibrium loading.

$$\frac{dq}{dt} = k(\downarrow)(q_{equilibrium}(\uparrow) - q(t)) \quad (13)$$

if $q_{equilibrium}$ increases, $k$ should decrease.

Decreasing the MST concentration or increasing the sorbate concentration should decrease the rate constant. However, the rate constant should not change with loading capacity since it is a constant. Therefore, the data reflects the rate of loading was controlled by diffusion to the MST (transport limited). Since both functions (Rhan and Ritchie) fitted the loading data on MST, we chose the Rhan function for fitting this data since this function includes transport rate limited adsorption. It was also observed that the Pu rate constant data as a function of the steady state Pu loading on MST shown in Fig. 8 (Rahn and Ritchie) revealed a significant noise

***Table 3.*** Sum of square error (SSE) values for the kinetic models

| Actinide | Initial concentration (μM) | MST (g/L) | 1st order | 2nd order | Elovich | Rhan | Ritchie | Power | Shrinking core model | Diffusion | Rudzinski |
|---|---|---|---|---|---|---|---|---|---|---|---|
| Pu | 0.0047 | 0.2 | 1.07 | 0.95 | 0.14 | 0.18 | 0.16 | 0.16 | 3.6 | 4.5 | 0.19 |
| | 0.0047 | 2 | 1.13 | 1.04 | 0.94 | 0.94 | 0.96 | 0.92 | 2.0 | 2.6 | 0.95 |
| | 0.04 | 0.2 | 0.88 | 0.81 | 1.02 | 1.1 | .33 | .48 | 6.1 | 5.6 | .24 |
| | 0.04 | 2 | 0.91 | 0.78 | 0.93 | 1.04 | .23 | 0.28 | 8.3 | 5.4 | .25 |
| | 1.17 | 0.2 | 1.24 | 1.33 | 1.48 | 1.65 | .26 | 0.32 | 5.6 | 7.0 | .31 |
| | 1.17 | 2 | 1.2 | 1.02 | 1.43 | 1.48 | .73 | 0.37 | 7.5 | 6.3 | .53 |
| | 0.7 | 0.2 | 1.0 | 0.32 | 0.438 | .62 | .48 | 0.84 | 17.2 | – | .35 |
| | 0.7 | 2 | 1.1 | 0.42 | 0.24 | .36 | .12 | 0.92 | 23.2 | – | .09 |
| U | 103 | 0.2 | 239 | 323 | 12 | 14 | 85 | 243 | 503 | 1044 | 78 |
| | 103 | 2 | 247 | 289 | 27 | 24 | 34 | 432 | 681 | – | 46 |
| | 62 | 0.2 | 122 | 341 | 16 | 15 | 63 | 428 | 285 | – | 55 |
| | 62 | 2 | 113 | 419 | 18 | 21 | 47 | 238 | 654 | – | 46 |
| | 38 | 0.2 | 44 | 410 | 38 | 48 | 38 | 298 | 284 | – | 48 |
| | 38 | 2 | 47 | 344 | 42 | 39 | 77 | 308 | 254 | – | 77 |

| | | | | | | | | | | | |
|---|---|---|---|---|---|---|---|---|---|---|---|
| Sr | 0.6 | 0.2 | 0.74 | 0.65 | 0.57 | .46 | .14 | .63 | 34 | 23 | .11 |
| | 0.6 | 2 | 0.81 | 0.78 | 0.78 | 1.4 | .80 | .78 | 58 | – | .84 |
| | 0.093 | 0.2 | 0.35 | 0.23 | 0.423 | .61 | .22 | .30 | 28 | – | .33 |
| | 0.093 | 2 | 0.49 | 0.24 | 0.43 | .72 | .20 | .44 | 42 | – | .23 |
| | 0.71 | 0.2 | 0.89 | 1.45 | 0.98 | .83 | 1.34 | .56 | 26 | – | 1.29 |
| | 0.71 | 2 | 0.76 | 1.91 | 0.84 | .79 | 1.88 | .38 | 18 | – | 1.67 |
| | 1.01 | 0.2 | 1.21 | 0.983 | 1.25 | 1.14 | .878 | 0.89 | 94 | – | .9 |
| | 1.01 | 2 | 1.34 | 0.824 | 0.825 | .91 | .674 | 0.68 | 48 | – | .66 |
| | 1.2 | 0.2 | 1.95 | 1.28 | 1.354 | 1.24 | 1.1 | 1.1 | 64 | – | .95 |
| | 1.2 | 2 | 1.9 | 1.44 | 3.49 | 2.78 | 1.12 | 1.29 | 83 | – | 1.2 |
| Np | 1.43 | 0.2 | 154 | 141 | 84 | 95 | 69 | 53 | 429 | 638 | 56 |
| | 1.43 | 2 | 198 | 134 | 184 | 168 | 79 | 143 | 934 | – | 79 |
| | 1.7 | 0.2 | 391 | 238 | 384 | 346 | 189 | 423 | 735 | – | 1787 |
| | 1.7 | 2 | 320 | 482 | 138 | 147 | 328 | 1032 | 748 | – | 330 |
| | 7.16 | 0.2 | 560 | 382 | 304 | 289 | 310 | 231 | 527 | – | 310 |
| | 7.16 | 2 | 501 | 427 | 348 | 329 | 419 | 487 | 763 | – | 411 |
| | 88.6 | 0.2 | 667 | 592 | 139 | 129 | 490 | 382 | 835 | – | 485 |
| | 88.6 | 2 | 495 | 236 | 354 | 388 | 200 | 428 | 934 | – | 198 |
| | 148 | 0.2 | 799 | 209 | 323 | 379 | 189 | 389 | 743 | – | 188 |
| | 148 | 2 | 813 | 1043 | 248 | 289 | 940 | 284 | 783 | – | 946 |

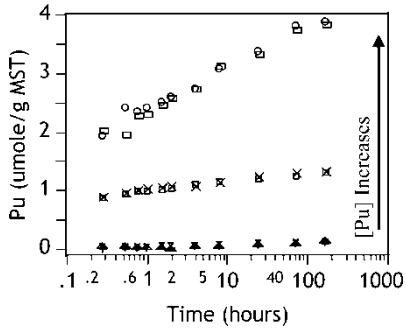


***Figure 6.*** Loading curve for Pu on MST under various conditions. Note all curves have the same initial slope or rate of loading.

(including bifurcation behavior) with the Ritchie's rate constant values, but not with the rate constant derived from the Rahn fitting function. Therefore, we selected the Rahn function to describe sorption on MST.

$$q_{Pu}(t) = \text{Loaded } Pu_{equilibrium} \lfloor 1 - e^{-k \times t^n} \rfloor \tag{14}$$

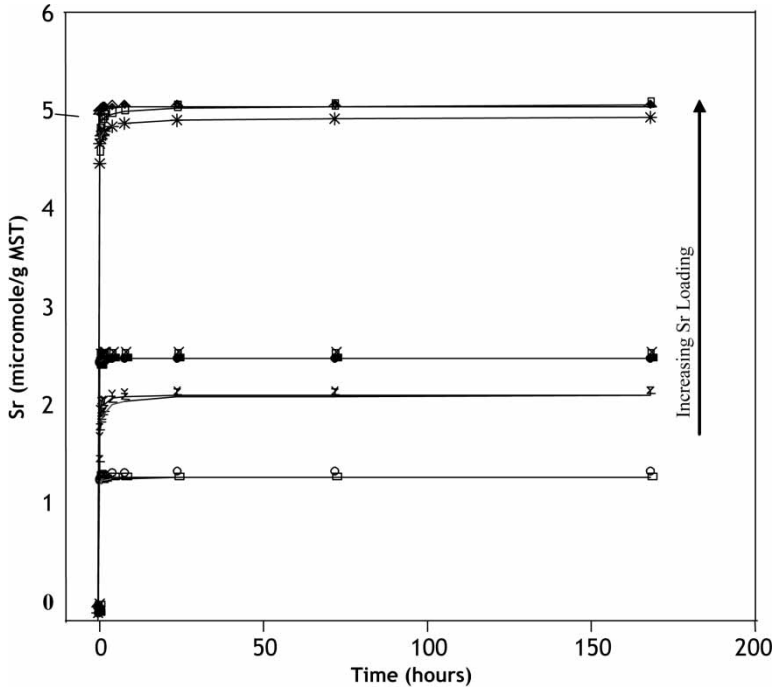


***Figure 7.*** The loading curves of Sr on MST under various conditions. Note identical slope for all the curves.

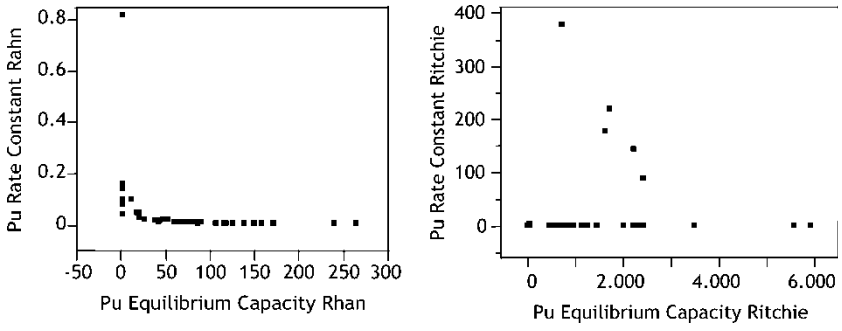


***Figure 8.*** The Pu rate constant data as a function of the steady state Pu loading on MST. The figure on the left is the Pu rate constant from the Rhan function and the figure on the right from the Ritchie function.



In this expression, $q_{Pu}(t)$ is the amount of plutonium loaded on MST (in units of micromole per grams of MST). The expression "Loaded $Pu_{equilibrium}$" is the equilibrium amount of plutonium on MST. The two parameters "$k$" and "$n$" were fitted against "Loaded $Pu_{equilibrium}$" parameter.

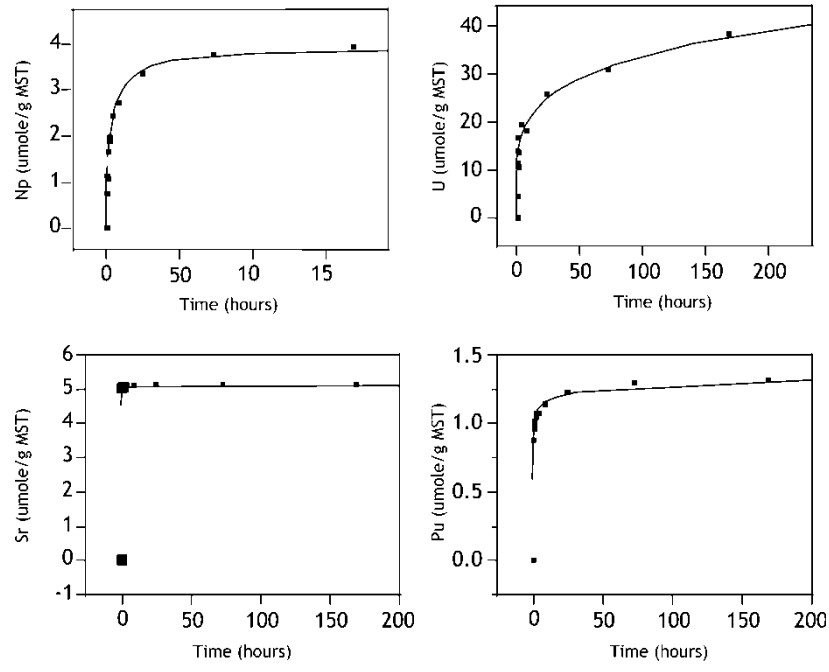


***Figure 9.*** A comparison between the Rhan function output and actinide loading data.

A sample of the fitting performance of the Rahn function is shown in the Fig. 9. A visual inspection of the figures in Fig. 9 shows the good fit between the Rahn function and the radionuclide sorption data on MST. From this fitting, the rate constant and another parameter associated with the Rahn function were derived. We also computed the sensitivity of these two (rate constant and exponent value) parameters derived from the Rahn function. The sensitivity of the Rhan function to variations of its parameters is shown in Fig. 10. The figures show the values of the parameters that minimized the sum of square errors (SSE). The figures clearly show that values for the rate constant and the exponent away from the minimum will not vary the SSE values significantly.

In order to predict sorption kinetics, we need to correlate the two parameters from Rahn's function (rate constant and exponent value) to the MST capacity for a given radionuclide.

We fitted the Rhan's rate constant as an inverse function of the equilibrium loading for all nuclide. The resulting fitting curves for Uranium and Plutonium is shown in Fig. 11. An inspection of Fig. 11 showed a good fit between both parameters from the Rhan function and the ultimately Pu and U loading. Similar fitting performance was obtained by fitting the Strontium and Neptunium loading data. The inverse relationship between the Rhan's parameter and the steady state loading is consistent with the expectation that the farther the system is away from equilibrium the faster the system approaches equilibrium initially. The fitted function provides the information needed to predict sorbate loading. The final loading functions for all sorbates follows.

Plutonium

$$k = \frac{0.207 \pm 0.4}{\text{Loaded } Pu_{equilibrium}} + 0.01 \pm 0.002 \tag{15}$$

$$n = \frac{1.71 \pm 0.8}{\text{Loaded } Pu_{equilibrium}} + 0.01 \pm 0.006 \tag{16}$$

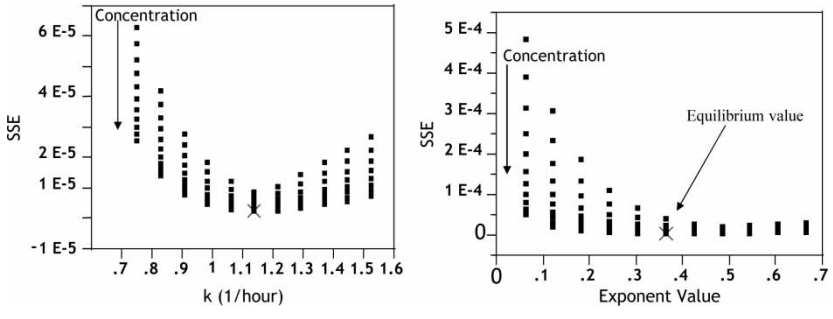


***Figure 10.*** The sensitivity plot of the two Rhan's function parameters to variations in the actinide concentration.

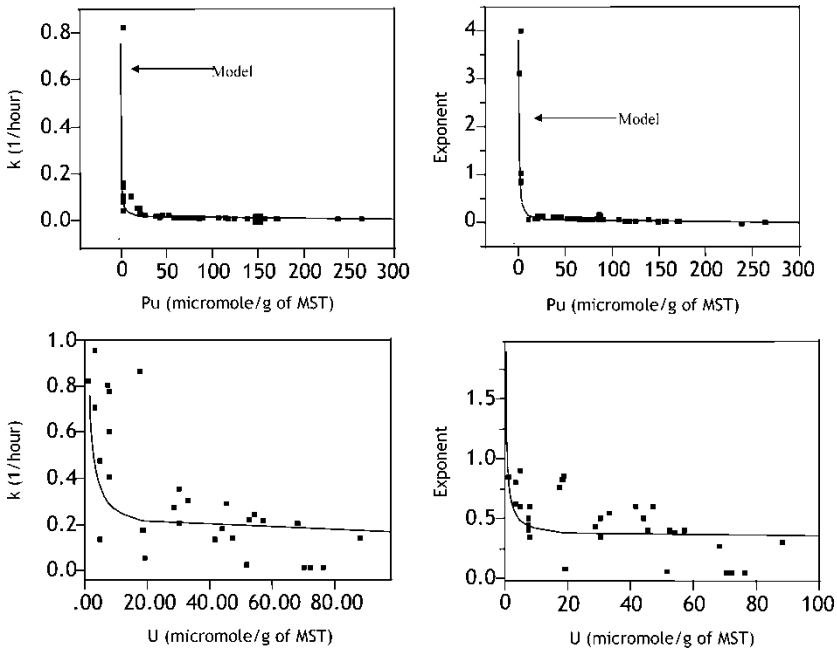


***Figure 11.*** A fit of the two parameters from Rhan's function as a function of actinide loading.



Strontium

$$k = \frac{-0.086 \pm 0.06}{\text{Loaded } Sr_{equilibrium}} + 4 \pm 0.6 \tag{17}$$

$$n = \frac{0.7 \pm 0.02}{\text{Loaded } Sr_{equilibrium}} + 0.36 \pm 0.13 \tag{18}$$

Uranium

$$k = \frac{1 \pm 0.34}{\text{Loaded } U_{equilibrium}} + 0.16 \pm 0.1 \tag{19}$$

$$n = \frac{0.7 \pm 0.4}{\text{Loaded } U_{equilibrium}} + 0.36 \pm 0.07 \tag{20}$$

Neptunium

$$k = \frac{2.1 \pm 0.4}{\text{Loaded } Np_{equilibrium}} + 0.11 \pm 0.12 \tag{21}$$

$$n = \frac{-0.26 \pm 0.1}{\text{Loaded } Np_{equilibrium}} + 0.55 \pm 0.3 \tag{22}$$

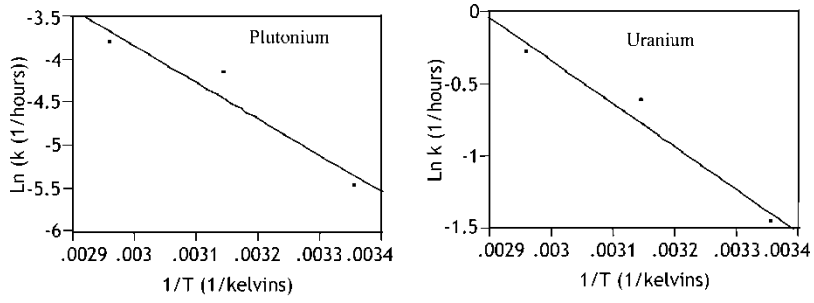


***Figure 12.*** The temperature dependency of one of the Rhan's function "*k*" for determining activation energies. The figure on the left is from the Uranium loading data. The figure on the right is from the Plutonium loading data.



## Temperature Effect

We fitted the temporal sorption data at different temperatures. We expect the rate constant to follow the Arhenius law as a function of temperature as shown in equation (23). Plotting the log of the rate constant (in the case of the Rhan function the constant is "*k*") as a function of the inverse of temperature should yield a linear trend. We found no statistical relationship between the other Rhan's parameter "*n*" and the inverse of temperature. The slope of the line gives the enthalpy energy for radionuclide sorption on MST. The intercept (at large temperature) yields the rate constant at room temperature. Fig. 12 provides plots of the rate constants as a function of temperature for Pu and U, respectively.

The slope of the lines in Fig. 14 yielded the activation energy for sorption. The activation energies measured 60 kJ/mol for Pu and 6.5 kJ/mol for U.

$$k = k_{room\ temperature} e^{-\Delta E/RT} \tag{23}$$

## CONCLUSIONS

The Dubinin-Astashov (DA) isotherm parameters for U, Pu, Sr, and Np have been updated to include additional data obtained since the original derivation. The DA isotherms were modified to include a kinetic function derived by Rahn to describe sorbate loading from the beginning of sorption up to steady state. The final functions describe both kinetic and thermodynamic sorption.

## REFERENCES

1. Fondeur, F.F., Hobbs, D.T., Barnes, M.J., and Fink, S.D. (2003) Sorption modeling of Sr, Pu, U, and Np adsorption on monosodium titanate. WSRC-TR-2003-00180.

2. Poirier, M.R., Herman, D.T., Burkett, P.R., Peters, T.B., Serkiz, S.M., and Fink, S.D. (2004) "Testing of the In situ mixed-iron oxide (ISMIO) alpha removal process. WSRC-TR-2004-00283.
3. Barnes, M.J., Fondeur, F.F., Hobbs, D.T., and Fink, S.D. (2004) Monosodium titanate multi-strike testing. WSRC-TR-2004-00145.
4. Azizian, S. (2004) Kinetics models of sorption: a theoretical analysis. *J. Coll. and Int. Sc.*, 276: 47–52.
5. Dubinin, M.M. and Radushkevich, L.V. (1947) Equation of the characteristic curve of activated charcoal. *Chem. Zentr.*, 1: 875.
6. (a) Cheung, C.W., Porter, J.F., and McKay, G. (2001) Sorption kinetic analysis for the removal of cadmium ions from effluents using bone char. *Wat. Res.*, 2001, 35: 605–612; (b) Forment, G.F. and Bischoff, K.B. (1990) *Chemical Reactor Analysis and Design*; John Wiley & Sons, Inc.
7. Rudzinski, W. and Panczyk, T. (2000) Kinetics of isothermal adsorption on energetically heterogeneous solid surfaces: a new theoretical description based on the statistical rate theory of interfacial transport. *J. Phys. Chem. B*, 104: 9149–9162.
8. Georgiadis, R., Peterlinz, K.P., and Peterson, A.W. (2000) Quantitative measurements and modeling of kinetics in nucleic acid monolayer films using SPR spectroscopy. *J. Am. Chem. Soc.*, 122: 3166–3173.
9. Sag, Y. and Aktay, Y. (2002) Kinetic studies on sorption of Cr(VI) and Cu(II) ions by chitin, chitosan, and rhizopus arrhizus. *Biochemical Eng. J.*, 12: 143–153.
10. Lazaridis, N.K. and Asouhidou, D.D. (2003) Kinetics of sorptive removal of chromium(VI) from aqueous solution by clacined Mg-Al-CO3 hydrotalcite. *Water Research*, 37: 2875–2882.
11. Hibbert, D.B., Gooding, J.J., and Erokhin, P. (2002) Kinetics of irreversible adsorption with diffusion: application to biomolecule immobilization. *Langmuir*, 18: 1770–1776.
12. Barlow, K., Nash, D., and Grayson, R. (2004) Investigating phosphorus interactions with bed sediments in a fluvial environment using a recirculating flume and intact soil cores. *Water Research*, 38: 3420–3430.
13. Fink, S.D., Hobbs, D.T., and Peters, T.B. (2002) Demonstration of MST efficacy on removal of actinides and strontium in bounding alpha waste. WSRC-TR-2002-00555.